

Validation of Custom Monte Carlo simulation of Light Transport in Scintillator

Hyunwoong Choi ^a, Kilyoung Ko ^a, Junhyeok Kim ^a, Wonku Kim ^a, Sangho Lee ^a, Youngsun Yi ^b, Gyuseong Cho ^{a*}

^aDepartment of Nuclear & Quantum Engineering, Korea Advanced Institute of Science and Technology (KAIST)
 291 Daehak-ro, Yuseong-gu, Daejeon, Korea, 34141

^bDepartment of Nuclear Engineering, Khalifa University

*Corresponding author : gscho1@kaist.ac.kr

1. Introduction

Scintillator crystals are widely used as radiation detector in wide range of field. The principle of scintillation detectors is counting scintillation light produced by ionizing radiation. Converting this light to electrical signal is needed so photodetectors such as photomultiplier tube (PMT) and avalanche photodiode (APD) are necessary [1].

Since the light propagation in the crystal and collecting the light at photodetector affects many parameters including energy resolution and timing resolution, it is important to understand how the light move inside the scintillator.

In this paper, we make our custom light transport Monte Carlo simulation inside of the scintillator and validate it with other results.

2. Methods and Results

2.1 Basic Theory of optical transport in scintillator

According to UNIFIED model, the surface is a collection of planar micro-facets. In this model, angle α is slope of the micro-facet deviated from mean normal vector n . The distribution of α is expressed as a normal distribution with mean value $\langle \alpha \rangle = 0$ and standard deviation σ_α . The other models such as backscattering and Lambertian reflection are independent of the roughness of surface. [2].

Polished surface is smooth surface that specular reflection occurs when a photon is reflected. Rough surface, in contrast, is a non-uniform surface that has many local micro-facet. When the light is reflected at rough surface, it leaves surface in a random direction.

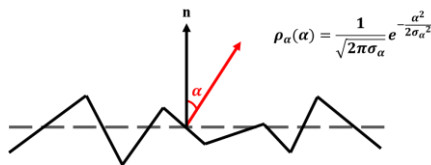


Fig.1. UNIFIED surface model

The probability of transmission and reflection for unpolarized light at the surface is determined by Fresnel's law (1) and Snell's law (2). R is the probability of reflection (the probability of refraction is $1-R$). θ_i and θ_t are incident and refraction angle respectively, n_1 and n_2 are refractive index of material. In case of $n_1 > n_2$, refraction angle cannot exceed 90° . We can calculate

critical angle that incident light suffers total internal reflection putting $\theta_t = 90^\circ$ into Eq. (2) [3].

$$R = \frac{1}{2} \left\{ \left(\frac{n_1 \cos \theta_i - n_2 \cos \theta_t}{n_1 \cos \theta_i + n_2 \cos \theta_t} \right)^2 + \left(\frac{n_1 \cos \theta_t - n_2 \cos \theta_i}{n_1 \cos \theta_t + n_2 \cos \theta_i} \right)^2 \right\} \quad (1)$$

$$\frac{\sin \theta_i}{\sin \theta_t} = \frac{n_1}{n_2} \quad (2)$$

Assume that the surface of crystal is polished, the initial angle of the light decides whether it is detected or not. The critical angle depends on the sort of the coupling materials to crystal such as air and optical grease. When initial angle of the light to photodetector surface is larger than critical angle, the light will disappeared by multiple reflections.

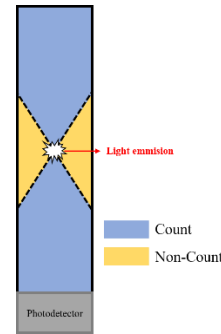


Fig.2. Light countable section in the crystal

The two types of reflectors are used widely, specular reflector (ESR, 3M) and Lambertian reflector (Teflon tape). Specular reflection is mirror-like reflection. The incident angle and the reflected angle is same.

Lambertian reflection is diffuse reflection that the direction of reflected light follows a cosine distribution regardless of incident angle. To generate cosine distribution for molecular flux, polar angular probability distribution is $\sin 2\theta$. More details about cosine law can see in [4].

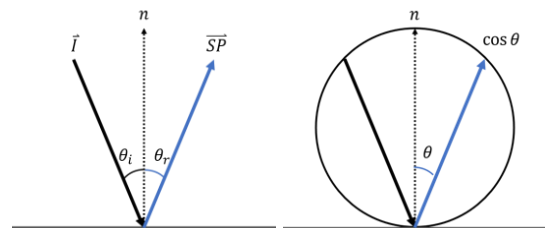


Fig.3. Specular reflection and lambertian reflection [4]

The temporal light emission distribution $p_{sc}(t)$ is expressed by linear combination of bi-exponential equation using rise time (τ_r) and decay time (τ_d) [5].

$$p_{sc}(t) = \begin{cases} \frac{1}{\tau_d - \tau_r} \left[e^{-\frac{(t-\theta)}{\tau_d}} - e^{-\frac{(t-\theta)}{\tau_r}} \right] & \text{if } t \geq 0 \\ 0 & \text{if } t < 0 \end{cases} \quad (3)$$

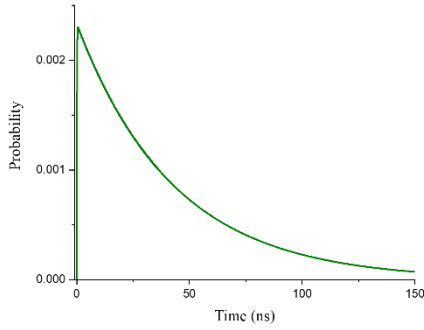


Fig.4. Temporal light emission of scintillator

Bulk absorption length (λ_{att}) means the distance when the probability has dropped to 1/e that a particle has not been absorbed. It is composed of scattering length (λ_{sc}) and absorption length (λ_{abs}) [6].

$$\frac{1}{\lambda_{att}} = \frac{1}{\lambda_{sc}} + \frac{1}{\lambda_{abs}} \quad (4)$$

2.2 Process of Monte Carlo Simulation

First step of Monte Carlo simulation is deciding crystal geometry, material, surface treatment, reflector type and γ -ray interact position. Next step is generating isotropic distributed and spontaneous light. Under coordinate system, the differential solid angle is $\sin \theta d\theta d\varphi$. The azimuth angle (φ) is distributed uniformly, but the polar angle (θ) is not. Using the Cumulative distribution function (CDF) of each angle and the random number (RN) between 0~1, we can simulate spontaneous and isotropic light generation. Since range of CDF is always 0~1, we can obtain specific angle by input RN to inverse function of CDF.

In case of polar angle, we can generate random polar angle following below equations.

$$\text{CDF}(\theta) = \frac{1}{2} (1 - \cos \theta) \quad [0 \leq \theta \leq \pi] \quad (5)$$

$$\theta = \cos^{-1}(1 - 2RN) \quad [0 \leq RN \leq 1] \quad (6)$$

Azimuth angle also can be generated in the same way.

$$\text{CDF}(\varphi) = \frac{\varphi}{2\pi} \quad [0 \leq \varphi \leq 2\pi] \quad (7)$$

$$\varphi = 2\pi RN \quad [0 \leq RN \leq 1] \quad (8)$$

Since polar and azimuth angle are determined from above equations, initial direction of light also determined by Eq. (10)

$$\vec{v} = (\sin \theta \cos \varphi, \sin \theta \sin \varphi, \cos \theta) \quad (9)$$

When the light generated with random direction with the initial position, it will arrive the nearest face in its direction. Whether the surface is in direction of the light can be simply determined by vector dot product calculation between surface normal vector and light direction vector. Because a surface acts like a plane in coordinate system, it is easy to calculate the distance between surface and photon.

The probability whether the light reflected or refracted at the surface calculated with the surface normal of randomly generated micro-facet. Reflected light will propagate to next nearest face with a new position and direction. Refracted light move to the reflector with refracted direction and its reflected direction depends on reflector type. When it re-enters to the crystal, its refracted direction is determined by the slope of randomly generated micro-facet. This iteration process stop when the light arrives at the surface that combines with photodetector.

After the light arrives at the detection surface, bulk absorption length and reflectivity of reflector are applied. Finally, we can get the total length the photon has moved within the scintillator. Total time of propagation can be obtained using speed of light and refractive index of crystal.

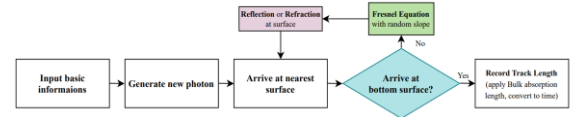


Fig.4. Brief overview of simulation flow chart

2.3 Simulation Result

A $3 \times 3 \times 20\text{mm}^3$ LYSO is modelled with 1.82 refractive index. Rise time and decay time of LYSO is 90ps and 430ns respectively. Also, we assume 138mm bulk absorption length at the peak wavelength of the emission spectrum of LYSO, 430nm.

The $3 \times 3\text{mm}^2$ photodetector is coupled to the crystal with optical grease (1.465 refractive index) and reflectors also coupled to crystal with air (1 refractive index). Reflectivity of the reflector is 98.5%. Polished surface is simulated with $\sigma_\alpha = 0.1^\circ$. Temporal light emission also simulated using CDF and random number.

We validate our custom Monte Carlo simulation by comparing the result of Cates. We can verify that our custom Monte Carlo simulation code is well-designed. Also in the convolution of two PDF, we can see the reverse of counts in specific time region according to height of interaction point.

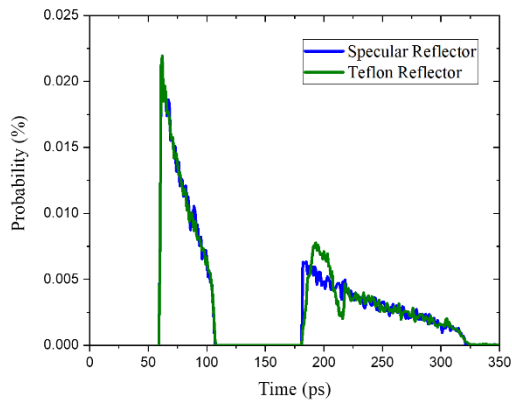


Fig.5. The probability of arrival time of photons at 10mm

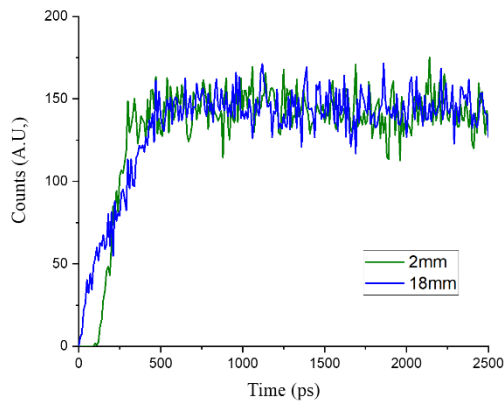


Fig.6. Convolution of light transport PDF and temporal emission profile.

3. Conclusions

In this paper, we show how to make custom light transport Monte Carlo simulation. And we validate our simulation is well matched with various references. With this Monte Carlo simulation, we can decide the most effective size, reflector type when designing the radiation detection system using scintillators.

However, the reflectivity is dependent on the wavelength of light and scintillators have a broad light emission spectrum. So only considering the peak wavelength overestimates light collection efficiency. In the future, we will consider the light emission spectrum of the scintillator and also simulate rough surface treatment according to the UNIFIED model.

ACKNOWLEDGEMENT

This research was supported by the KAI-NEET Institute (or the KAIST-KU Joint Research Center), KAIST, Korea and (other funding organization if any)

REFERENCES

- [1] G. F. Knoll, Radiation Detection and Measurement, John Wiley & Sons, New York, 2010
- [2] Nayar S K, Ikeuchi K, and Kanade T, "Surface Reflection: Physical and Geometrical Perspectives", The Robotics Institute, Carnegie Mellon University, Pittsburgh, Pennsylvania, March 1989
- [3] Yang X, Downie E, Farrell T and Peng H, Study of light transport inside scintillation crystals for PET detectors Phys. Med. Biol. 58 pp 2144–61, 2013
- [4] J Greenwood, The correct and incorrect generation of a cosine distribution of scattered particles for Monte-Carlo modelling of vacuum, Vacuum, Volume 67, Issue 2, Pages 217-222, 2002
- [5] Analytical calculation of the lower bound on timing resolution for PET scintillation detectors comprising high-aspect-ratio crystal elements Joshua W Cates et al, Phys. Med. Biol. 2015
- [6] Moisan C, Vozza D and Loope M, Simulating the performances of an LSO based position encoding detector for PET IEEE Nucl. Sci. Symp. Conf. Record 2 1211–5, 1996